2026 IEEE International Conference on Robotics and Automation (ICRA 2026)
June 1-5, 2026. Vienna, Austria

Two-Time-Scale Composite Learning Online Identification and Control for Compliant-Joint Robots

Tian Shi[1], Lin Liu[2], Qian Wang[3], Jinya Su[1], Shihua Li[1], and Yongping Pan[1]

Abstract— **SP-based synthesis yields two-time-scale control that allows compliant-joint robots to achieve high-quality tracking at low implementation cost. Composite learning enables exact online identification and control of robots without the stringent condition known as persistent excitation (PE). However, to achieve exact online identification for compliant-joint robots, parameter update derived from SP-based synthesis and composite learning requires physically unavailable states. This paper presents a novel SP-based composite learning robot control (SP-CLRC) strategy for compliant-joint robots that achieves exact online identification and control without requiring access to physically unavailable states. In the proposed method, link-side and actuator-side parameters are estimated separately, enabling exact online identification using available robot states. A two-time-scale composite learning method is proposed to guarantee practical exponential stability of the closed-loop system with parameter convergence under interval excitation, a condition strictly weaker than PE. Experiments on a two-degree-of-freedom robot driven by series elastic actuators have shown that the proposed SP-CLRC significantly outperforms the baseline in online identification and tracking accuracy.**

I. Introduction

Compliant-joint robots employ elastic elements, such as series elastic actuators (SEAs), to decouple actuator inertia from link inertia [1]. Compared with traditional rigid-joint robots, compliant-joint robots exhibit several attractive features, such as natural motion, intrinsic compliance, and backdrivability [2]. Meanwhile, elastic elements may induce oscillations, increase settling times, or even destroy closed-loop stability during robot control [3]. Compliant-joint robots with constant joint stiffness can be expressed by a flexible-joint robot (FJR) model, thereby allowing joint compliance to be respected during the control design. Typical control approaches of FJRs include backstepping-type control [4]–[7], disturbance observer-based control [8]–[10], and passivity-based control [11]–[14], where physical experiments are provided in all these results. However, most of these results rely on exact model information or require estimating robot accelerations and jerks, which is difficult and usually sensitive to measurement noise.

Singular perturbation (SP)-based control reformulates the full-order FJR model into a two-time-scale form, consisting of slow and fast subsystems, from which reduced and boundary-layer systems are derived, respectively [15]. SP-based synthesis facilitates the design of FJR control laws without involving the higher-order time derivatives, such as robot accelerations and jerks. Moreover, compared with alternative FJR control approaches, SP-based control has the lowest implementation cost because its controller complexity is equivalent to that of its rigid-robot counterpart [16]. From the SP principle, the (practical exponential) stability of the full-order system requires both reduced and boundary-layer systems being exponentially stable [15]. Achieving the exponential stability of the boundary-layer system is relatively simple, and proportional-derivative (PD) control is usually sufficient, whereas most control methods for the reduced system rely on accurate robot models to ensure exponential stabilization [17]–[20].

Composite learning robot control (CLRC) is an innovative adaptive control framework that exploits memory regressor extension to boost parameter estimation [21]. Compared with the classical adaptive robot control, CLRC can achieve exponential stability with parameter convergence under interval excitation (IE), a condition strictly weaker than persistent excitation (PE) [22]. CLRC has been combined with SP-based synthesis for compliant-joint robots with high degrees of freedom (DoFs) to achieve high-quality tracking under model uncertainties [23], [24], where an identifiable parameter vector that couples link-side and actuator-side parameters is estimated online using a regression equation of the reduced system. Nevertheless, the methods in [23], [24] require physically inaccessible states of the reduced system for exact online identification, and directly replacing these states with available robot states may degrade identification accuracy because these two states are fundamentally different [23]. This problem arises in all SP-based FJR adaptive control methods, including [25].

Motivated by the above investigation, this article proposes a novel SP-based CLRC (SP-CLRC) for compliant-joint robots to achieve exact online identification and control without requiring physically unavailable states. In the proposed method, a PD torque controller is used to establish exponential stability of the boundary-layer system, and an adaptive position controller with two composite learning laws is designed to estimate link-side and actuator-side parameters separately, so exponential stability of the reduced system with parameter convergence is achieved under the weakened IE condition. Experiments on a two-DoF SEA-driven robot are carried out to validate the proposed method. Compared to existing SP-based adaptive control results of compliant-joint robots such as [23]–[25], the major novelties of this study lie in two aspects: 1) The two-time-scale composite learning is developed to achieve exact online identification by using available robot states; 2) a novel SP-CLRC law is proposed to achieve superior exponential

*Corresponding Author: Yongping Pan.
[1]Tian Shi, Jinya Su, Shihua Li, and Yongping Pan are with the School of Automation, Southeast University, Nanjing 210096, China {shitian, sucas,lsh,panyp}@seu.edu.cn
[2]Lin Liu is with the School of Advanced Manufacturing, Sun Yat-sen University, Shenzhen 518100, China liulin67@mail.sysu.edu.cn
[3]Qian Wang is with the School of Intelligent Systems Engineering, Sun Yat-sen University, Shenzhen 518107, China wangq666@mail2.sysu.edu.cn

tracking under the weakened IE condition.

II. Problem Formulation

Consider an n-DoF FJR model as follows [26]:

$$M(\boldsymbol{q})\ddot{\boldsymbol{q}} + C(\boldsymbol{q},\dot{\boldsymbol{q}})\dot{\boldsymbol{q}} + G(\boldsymbol{q}) + F(\dot{\boldsymbol{q}}) = \boldsymbol{\tau}_{\rm a}, \tag{1}$$

$$B\ddot{\boldsymbol{\theta}} + \boldsymbol{\tau}_{\rm a} = \boldsymbol{u}, \boldsymbol{\tau}_{\rm a} = \boldsymbol{\tau} + DK^{-1}\dot{\boldsymbol{\tau}} \tag{2}$$

in which $\boldsymbol{q}(t) := [q_1(t), q_2(t), \cdots, q_n(t)]^T \in \mathbb{R}^n$ is a joint position, $\boldsymbol{\theta}(t) := [\theta_1(t), \theta_2(t), \cdots, \theta_n(t)]^T \in \mathbb{R}^n$ is a motor position, $\boldsymbol{\tau}_{\rm a}(t) \in \mathbb{R}^n$ is an actuation torque, $\boldsymbol{\tau}(t) := K(\boldsymbol{\theta} - \boldsymbol{q}$ is a spring torque, and $\boldsymbol{u}(t) \in \mathbb{R}^n$ is a motor torque; $M(\boldsymbol{q}) \in \mathbb{R}^{n\times n}$, $C(\boldsymbol{q},\dot{\boldsymbol{q}}) \in \mathbb{R}^{n\times n}$, $G(\boldsymbol{q}) \in \mathbb{R}^n$, and $F(\dot{\boldsymbol{q}}) \in \mathbb{R}^n$ are an inertia matrix, a centripetal-Coriolis matrix, a gravitational vector, and a friction vector of the rigid link dynamics (1), respectively, and $B \in \mathbb{R}^{n\times n}$, $D \in \mathbb{R}^{n\times n}$, and $K \in \mathbb{R}^{n\times n}$ are inertia, damping, and stiffness matrices of the compliant actuator dynamics (2), respectively. Note that $\boldsymbol{q}$, $\dot{\boldsymbol{q}}$, $\boldsymbol{\tau}$, $\dot{\boldsymbol{\tau}}$, $\boldsymbol{\theta}$, and $\dot{\boldsymbol{\theta}}$ are measurable. Some useful properties from [26] and definitions from [27] are presented as follows.

Property 1: $M(\boldsymbol{q})$ is a symmetric positive-definite matrix that satisfies $m_0\|\boldsymbol{x}\|^2 \le \boldsymbol{x}^T M(\boldsymbol{q})\boldsymbol{x} \le \bar{m}\|\boldsymbol{x}\|^2$, $\forall \boldsymbol{x} \in \mathbb{R}^n$, and B, D and K are positive-definite, diagonal, and constant matrices, where $m_0, \bar{m} \in \mathbb{R}^+$ are some constants.

Property 2: $\dot{M}(\boldsymbol{q}) - 2C(\boldsymbol{q},\dot{\boldsymbol{q}})$ is skew-symmetric such that $\boldsymbol{x}^T(\dot{M}(\boldsymbol{q}) - 2C(\boldsymbol{q},\dot{\boldsymbol{q}}))\boldsymbol{x} = 0$, $\forall \boldsymbol{x} \in \mathbb{R}^n$.

Property 3: The left-hand side of (1) can be converted into a linearly parameterized form as follows:

$$M(\boldsymbol{q})\dot{\boldsymbol{v}} + C(\boldsymbol{q},\dot{\boldsymbol{q}})\boldsymbol{v} + G(\boldsymbol{q}) + F(\dot{\boldsymbol{q}}) = \Phi^T(\boldsymbol{q},\dot{\boldsymbol{q}},\boldsymbol{v},\dot{\boldsymbol{v}})W \tag{3}$$

where $\boldsymbol{v}(t) \in \mathbb{R}^n$ is an auxiliary variable, $\Phi : \mathbb{R}^{4n} \mapsto \mathbb{R}^{N\times n}$ is a smooth regression matrix (i.e., regressor), and $W \in \mathbb{R}^N$ is a link-side base parameter vector.

Definition 1: A bounded signal $\Phi(t) \in \mathbb{R}^{N\times n}$ is of PE, if $\exists \sigma, \varsigma_{\rm e} \in \mathbb{R}^+$ to get $\int_{t-\varsigma_{\rm e}}^{t} \Phi(\varsigma)\Phi^T(\varsigma)d\varsigma \ge \sigma I, \forall t \ge 0$.

Definition 2: A bounded signal $\Phi(t) \in \mathbb{R}^{N\times n}$ is of IE at $t = t_{\rm e}$, if $\exists\ \sigma, \varsigma_{\rm e}, t_{\rm e} \in \mathbb{R}^+$ to get $\int_{t_{\rm e}-\varsigma_{\rm e}}^{t_{\rm e}} \Phi(\varsigma)\Phi^T(\varsigma)d\varsigma \ge \sigma I$.

Let $\boldsymbol{q}_{\rm d}(t) := [q_{\rm d1}(t), q_{\rm d2}(t), \cdots, q_{{\rm d}n}(t)]^T \in \mathbb{R}^n$ denote the desired output. Define tracking errors $\boldsymbol{e}_1(t) := \boldsymbol{q}_{\rm d}(t) - \boldsymbol{q}(t)$ and $\boldsymbol{e}_2(t) := \dot{\boldsymbol{q}}_{\rm r}(t) - \dot{\boldsymbol{q}}(t) = \dot{\boldsymbol{e}}_1(t) + \Lambda\boldsymbol{e}_1(t)$ with $\dot{\boldsymbol{q}}_{\rm r}(t) := \dot{\boldsymbol{q}}_{\rm d}(t) + \Lambda\boldsymbol{e}_1(t)$, where $\Lambda \in \mathbb{R}^{n\times n}$ is a control gain matrix that is positive-definite and diagonal. The objective of this study is to develop a novel control strategy for the FJR system (1)–(2) to achieve exact online identification and tracking control using physically available robot states.

III. Singular Perturbation Formulation

Since the joint torque $\boldsymbol{\tau}$ is physically measurable in many compliant-joint robots, it is natural to reformulate the actuator dynamics (2) into an equation on $\boldsymbol{\tau}$ as follows:

$$K^{-1}B\ddot{\boldsymbol{\tau}} + K^{-1}D\dot{\boldsymbol{\tau}} + \boldsymbol{\tau} = \boldsymbol{u} - B\ddot{\boldsymbol{q}}. \tag{4}$$

Let $K = K_0/\epsilon^2$ and $D = D_0/\epsilon$ with $K_0, D_0 \in \mathcal{O}(1)$ and $0 < \epsilon \ll 1$, in which $\boldsymbol{x} \in \mathcal{O}(1)$ represents $\boldsymbol{x} \in \mathbb{R}^{n\times n}$ being of the order 1. Note that K_0, D_0, and ϵ are introduced solely for theoretical analysis and do not appear in the actual control law $\boldsymbol{u}$ [28]. It follows from (4) to obtain

$$\epsilon^2 B\ddot{\boldsymbol{\tau}} + \epsilon D_0\dot{\boldsymbol{\tau}} + K_0\boldsymbol{\tau} = K_0(\boldsymbol{u} - B\ddot{\boldsymbol{q}}). \tag{5}$$

Multiplying (5) by B^{-1} and using the expression of $\ddot{\boldsymbol{q}}$ from (1) to the resulting equality, one gets

$$\begin{aligned}&\epsilon^2\ddot{\boldsymbol{\tau}} + (M^{-1}(\boldsymbol{q}) + B^{-1})(\epsilon D_0\dot{\boldsymbol{\tau}} + K_0\boldsymbol{\tau})\\ =&K_0(B^{-1}\boldsymbol{u} + M^{-1}(\boldsymbol{q})\left(C(\boldsymbol{q},\dot{\boldsymbol{q}})\dot{\boldsymbol{q}} + G(\boldsymbol{q}) + F(\dot{\boldsymbol{q}})\right)).\end{aligned} \tag{6}$$

Differentiating $\boldsymbol{e}_2$ on t, multiplying the resulting expression by $M(\boldsymbol{q})$, and substituting $\ddot{\boldsymbol{q}}$ from (1) yield

$$M(\boldsymbol{q})\dot{\boldsymbol{e}}_2 = M(\boldsymbol{q})\ddot{\boldsymbol{q}}_{\rm r} + C(\boldsymbol{q},\dot{\boldsymbol{q}})\dot{\boldsymbol{q}} + G(\boldsymbol{q}) + F(\dot{\boldsymbol{q}}) - \boldsymbol{\tau}_{\rm a}. \tag{7}$$

The FJR system (1) with (2) can be reformulated into a SP form by using (6) and (7) as follows:

$$\begin{cases} \dot{\boldsymbol{e}} = \boldsymbol{f}(t,\boldsymbol{e},\boldsymbol{y}),\ \boldsymbol{e}(0) = \boldsymbol{e}_0 \\ \epsilon\dot{\boldsymbol{y}} = \boldsymbol{g}(t,\boldsymbol{e},\boldsymbol{y}),\ \boldsymbol{y}(0) = \boldsymbol{y}_0 \end{cases} \tag{8}$$

with $\boldsymbol{e}_0, \boldsymbol{y}_0 \in \mathbb{R}^{2n}$, where $\boldsymbol{e} := [\boldsymbol{e}_1^T, \boldsymbol{e}_2^T]^T$ is a slow variable of the slow time-scale subsystem, $\boldsymbol{y} := [\boldsymbol{y}_1^T, \boldsymbol{y}_2^T]^T = [\boldsymbol{\tau}^T, \epsilon\dot{\boldsymbol{\tau}}^T]^T$ is a fast variable of the fast time-scale subsystem, and the expressions of $\boldsymbol{f}, \boldsymbol{g} : \mathbb{R}^+ \times \mathbb{R}^{2n} \times \mathbb{R}^{2n} \mapsto \mathbb{R}^{2n}$ are straightforward to obtain so they are omitted here.

Following the derivations in [23], one obtains an open-loop reduced system by making $\epsilon = 0$ in (8) as follows[1]:

$$\begin{aligned}(M(\bar{\boldsymbol{q}}) + B)\dot{\bar{\boldsymbol{e}}}_2 =&(M(\bar{\boldsymbol{q}}) + B)\ddot{\bar{\boldsymbol{q}}}_{\rm r} + C(\bar{\boldsymbol{q}},\dot{\bar{\boldsymbol{q}}})\dot{\bar{\boldsymbol{q}}}\\ &+ G(\bar{\boldsymbol{q}}) + F(\dot{\bar{\boldsymbol{q}}}) - \boldsymbol{u}_{\rm s}\end{aligned} \tag{9}$$

where $\boldsymbol{u}_{\rm s} \in \mathbb{R}^n$ denotes a *slow controller*, and the superscript "–"[2] implies that the corresponding variable is defined in the case of $\epsilon = 0$. Let $t_\epsilon := t/\epsilon$ be a *"stretched" time variable*. Define a virtual torque error $\boldsymbol{z}(t_\epsilon) := \boldsymbol{\tau}(t) - \boldsymbol{\tau}_{\rm qss} \in \mathbb{R}^n$, where $\boldsymbol{\tau}_{\rm qss} := \boldsymbol{u}_{\rm s} - B\ddot{\boldsymbol{q}}_{\rm r} + B\dot{\boldsymbol{e}}_2 \in \mathbb{R}^n$ is a quasi-steady-state value of $\boldsymbol{\tau}$ [15]. Similar to [23], changing the time scale of the system (8) from t to t_ϵ and setting $\epsilon = 0$, one obtains an open-loop boundary-layer system of (8) as follows:

$$\boldsymbol{z}'' + (M^{-1}(\boldsymbol{q}) + B^{-1})(D_0\boldsymbol{z}' + K_0\boldsymbol{z}) = K_0B^{-1}\boldsymbol{u}_{\rm f} \tag{10}$$

with $\boldsymbol{z}' := d\boldsymbol{z}/dt_\epsilon$, where $\boldsymbol{u}_{\rm f} := \boldsymbol{u} - \boldsymbol{u}_{\rm s}$ is a *fast controller*.

According to the *extended Tikhonov's theorem* [15, Th. 11.2], if there exist a slow controller $\boldsymbol{u}_{\rm s}$ and a fast controller $\boldsymbol{u}_{\rm f}$ such that the reduced system (9) and the boundary-layer system (10) achieve exponential stability, respectively, then the full-order system (1)–(2) achieves practical exponential stability under the following integrated control law [25]:

$$\boldsymbol{u}(t,\boldsymbol{e},\boldsymbol{y}) = \boldsymbol{u}_{\rm lin}(t,\boldsymbol{e}) + \boldsymbol{u}_{\rm act}(\boldsymbol{y}) \tag{11}$$

in which $\boldsymbol{u}_{\rm lin} \in \mathbb{R}^n$ denotes a position controller for the rigid link dynamics (1), and $\boldsymbol{u}_{\rm act} \in \mathbb{R}^n$ denotes a torque controller for the compliant actuator dynamics (2). The linearity of the

[1] Setting $\epsilon = 0$ is intended to derive the fast and slow time-scale subsystems, which are used to approximate the full-order system (8). This is a standard procedure in SP control design and is solely for theoretical analysis.

[2] The superscript "–" is omitted subsequently to simplify presentation, but the variables $\bar{\boldsymbol{q}}$ in (9) and $\boldsymbol{q}$ in (1) are fundamentally different.

boundary-layer system (10) allows exponential stability to be achieved easily by a PD torque controller

$$\boldsymbol{u}_{\rm act} = -K_{\rm p}\boldsymbol{\tau} - \epsilon K_{\rm d}\dot{\boldsymbol{\tau}} \tag{12}$$

with $K_{\rm p}, K_{\rm d} \in \mathbb{R}^{n\times n}$ being positive-definite and diagonal control gain matrices. Making $\epsilon = 0$ in (11) yields

$$\boldsymbol{u}_{\rm s} = \boldsymbol{u}_{\rm lin}(t,\boldsymbol{e}) - K_{\rm p}\boldsymbol{\tau}_{\rm qss}. \tag{13}$$

It follows from $\boldsymbol{u}_{\rm f} = \boldsymbol{u} - \boldsymbol{u}_{\rm s}$, (11), and (13) that

$$\boldsymbol{u}_{\rm f} = -K_{\rm p}\boldsymbol{z} - \epsilon K_{\rm d}\dot{\boldsymbol{\tau}}. \tag{14}$$

Applying (14) to (10) yields a new boundary-layer system

$$\begin{aligned}&\boldsymbol{z}'' + K_0 B^{-1}((I + BM^{-1}(\boldsymbol{q}))K_0^{-1}D_0 + K_{\rm d})\boldsymbol{z}'\\ =& -K_0 B^{-1}((I + BM^{-1}(\boldsymbol{q})) + K_{\rm p})\boldsymbol{z}\end{aligned} \tag{15}$$

which is linear time-invariant in the time scale t_ϵ, such that its global exponential stability can be guaranteed by setting reasonable $K_{\rm p}$ and $K_{\rm d}$ [24]. It is worth noting that the reduced system (9) and the boundary-layer system (10) are employed solely for preliminary analysis, and their specific expressions depend on the choice of the control law $\boldsymbol{u}$ in (11).

IV. Composite Learning Robot Control

This section first establishes the exponential stability of the reduced system (9), followed by the SP-CLRC design for the full-order system (1)–(2). Solving (13) with respect to $\boldsymbol{u}_{\rm s}$ using the expression of $\boldsymbol{\tau}_{\rm qss}$ under (13), one obtains

$$\boldsymbol{u}_{\rm s} = (I + K_{\rm p})^{-1}\left(\boldsymbol{u}_{\rm lin} - K_{\rm p}B(\dot{\boldsymbol{e}}_2 - \ddot{\boldsymbol{q}}_{\rm r})\right). \tag{16}$$

Design the link-side position controller

$$\boldsymbol{u}_{\rm lin}(t,\boldsymbol{e}) = (I + K_{\rm p})\boldsymbol{\tau}_{\rm r} \tag{17}$$

where $\boldsymbol{\tau}_{\rm r} \in \mathbb{R}^n$ can be any rigid robot control law. Applying (17) to (11), one gets the final control law

$$\boldsymbol{u}(\boldsymbol{\tau}_{\rm r}, \boldsymbol{y}) = \boldsymbol{\tau}_{\rm r} - K_{\rm p}(\boldsymbol{\tau} - \boldsymbol{\tau}_{\rm r}) - \epsilon K_{\rm d}\dot{\boldsymbol{\tau}} \tag{18}$$

where $\boldsymbol{\tau}_{\rm r}$ serves as a reference torque. Applying (16) and (17) to (9) and substituting the definition of $\boldsymbol{e}_2$ in Sec. II into the resulting expression, one obtains

$$M_{\rm e}(\boldsymbol{q})\ddot{\boldsymbol{q}} + C(\boldsymbol{q},\dot{\boldsymbol{q}})\dot{\boldsymbol{q}} + G(\boldsymbol{q}) + F(\dot{\boldsymbol{q}}) = \boldsymbol{\tau}_{\rm r} \tag{19}$$

where $M_{\rm e}(\boldsymbol{q}) := M(\boldsymbol{q}) + B_{\rm e} \in \mathbb{R}^{n\times n}$ is a generalized inertia matrix for the reduced system (19), and $B_{\rm e} := (I + K_{\rm p})^{-1}B \in \mathbb{R}^{n\times n}$ is a diagonal matrix of shaped actuator inertia. Then, one has the following property of (19) [24].

Property 4: The left-hand side of (19) can be expressed into a linearly parameterized formula as follows:

$$M_{\rm e}(\boldsymbol{q})\dot{\boldsymbol{v}} + C(\boldsymbol{q},\dot{\boldsymbol{q}})\boldsymbol{v} + G(\boldsymbol{q}) + F(\dot{\boldsymbol{q}}) = \Psi^T(\boldsymbol{q},\dot{\boldsymbol{q}},\boldsymbol{v},\dot{\boldsymbol{v}})W_{\rm e} \tag{20}$$

where $\boldsymbol{v}(t) \in \mathbb{R}^n$ is an auxiliary variable, $\Psi : \mathbb{R}^{4n} \mapsto \mathbb{R}^{N_{\rm e}\times n}$ is an extended smooth regressor, $W_{\rm e} \in \mathbb{R}^{N_{\rm e}}$ is an extended parameter vector, and $N_{\rm e}$ is the number of all parameters.

Design the adaptive position control law

$$\boldsymbol{\tau}_{\rm r} = K_{\rm c}\boldsymbol{e}_2 + \Psi^T(\boldsymbol{q},\dot{\boldsymbol{q}},\dot{\boldsymbol{q}}_{\rm r},\ddot{\boldsymbol{q}}_{\rm r})\hat{W}_{\rm e} \tag{21}$$

in which $K_{\rm c} \in \mathbb{R}^{n\times n}$ is a positive-definite diagonal matrix of control gains, and $\hat{W}_{\rm e}(t) \in \mathbb{R}^{N_{\rm e}}$ is an estimate of $W_{\rm e}$. In general, the parameter vector $W_{\rm e}$ can be estimated online by using CLRC and the regression equation (20) with $\boldsymbol{v} = \dot{\boldsymbol{q}}$, and exponential stability of the closed-loop system with parameter convergence can be established under the IE condition. However, in such a control design, the physically unavailable states $\bar{\boldsymbol{q}}$ and $\dot{\bar{\boldsymbol{q}}}$ in the reduced system (19) must be applied to achieve the parameter estimaton error $\tilde{W}_{\rm e} := W_{\rm e} - \hat{W}_{\rm e}(t)$ converging to $\boldsymbol{0}$. So in practical applications, $\bar{\boldsymbol{q}}$ and $\dot{\bar{\boldsymbol{q}}}$ are replaced by the measurable states $\boldsymbol{q}$ and $\dot{\boldsymbol{q}}$, which may degrade estimation accuracy, and in turn reduce tracking accuracy [23].

The parameter vector $W_{\rm e}$ in (20) comprises the link-side base parameter W in (3) and the actuator inertia parameter B in (2), such that it can be obtained by using the rigid link dynamics (1) and the compliant actuator dynamics (2) to estimate W and B, respectively. Applying (3) with $\boldsymbol{v} = \dot{\boldsymbol{q}}$ to (1), one obtains a link-side regression equation

$$\boldsymbol{\tau}_{\rm a}(t) = \Phi^T(\boldsymbol{q},\dot{\boldsymbol{q}},\dot{\boldsymbol{q}},\ddot{\boldsymbol{q}})W. \tag{22}$$

Since the joint acceleration $\ddot{\boldsymbol{q}}$ is immeasurable, a low-pass filter $L_\alpha(s) := \frac{\alpha}{s+\alpha}$ is applied to (22) such that

$$\boldsymbol{\tau}_{\rm af}(t) = \Phi_{\rm f}^T(\boldsymbol{q},\dot{\boldsymbol{q}})W \tag{23}$$

where $\Phi_{\rm f}(\boldsymbol{q},\dot{\boldsymbol{q}}) := \alpha e^{-\alpha t} * \Phi(\boldsymbol{q},\dot{\boldsymbol{q}},\dot{\boldsymbol{q}},\ddot{\boldsymbol{q}})$ and $\boldsymbol{\tau}_{\rm af} := \alpha e^{-\alpha t} * \boldsymbol{\tau}_{\rm a}$ denote filtered counterparts of $\Phi(\boldsymbol{q},\dot{\boldsymbol{q}},\dot{\boldsymbol{q}},\ddot{\boldsymbol{q}})$ and $\boldsymbol{\tau}_{\rm a}$, respectively, $\alpha \in \mathbb{R}^+$ is a filtering constant, s is the complex variable of Laplace transformation, and "$*$" is the convolution operator [29]. A torque prediction model is given by

$$\hat{\boldsymbol{\tau}}_{\rm af}(t) = \Phi_{\rm f}^T(\boldsymbol{q},\dot{\boldsymbol{q}})\hat{W}(t) \tag{24}$$

where $\hat{\boldsymbol{\tau}}_{\rm af}(t) \in \mathbb{R}^n$ is a predicted value of $\boldsymbol{\tau}_{\rm af}$. Let

$$\Theta(t) := \int_{t-\varsigma_{\rm e}}^{t} \Phi_{\rm f}(\varsigma)\Phi_{\rm f}^T(\varsigma)d\varsigma \tag{25}$$

with $\Phi_{\rm f}(t) = \Phi_{\rm f}(\boldsymbol{q},\dot{\boldsymbol{q}})$ for short and $\varsigma_{\rm e} \in \mathbb{R}^+$ being an integral duration. Multiplying (23) by $\Phi_{\rm f}$, integrating the result at $[t - \varsigma_{\rm e}, t]$, and using (25), one obtains

$$\Theta(t)W = \int_{t-\varsigma_{\rm e}}^{t} \Phi_{\rm f}(\varsigma)\boldsymbol{\tau}_{\rm af}(\varsigma)d\varsigma := \boldsymbol{\varphi}(t). \tag{26}$$

It is assumed that there exist certain constants $\sigma, \varsigma_{\rm e}, t_{\rm e} \in \mathbb{R}^+$ so that the IE condition $\Theta(t_{\rm e}) \geq \sigma I$ in Definition 2 is satisfied. To take full advantage of excitation information for parameter estimation, define a torque prediction error

$$\boldsymbol{\varepsilon}(t) := \boldsymbol{\tau}_{\rm af}(t) - \Phi_{\rm f}^T\hat{W}(t) \tag{27}$$

and a generalized torque prediction error

$$\boldsymbol{\xi}(t) := \begin{cases} \boldsymbol{\varphi}(t) - \Theta(t)\hat{W}(t), & t < t_{\rm e} \\ \boldsymbol{\varphi}(t_{\rm e}) - \Theta(t_{\rm e})\hat{W}(t), t \geq t_{\rm e} \end{cases}. \tag{28}$$

Design a link-side composite learning law

$$\dot{\hat{W}} = \Gamma(\Phi(\boldsymbol{q},\dot{\boldsymbol{q}},\dot{\boldsymbol{q}}_{\rm r},\ddot{\boldsymbol{q}}_{\rm r})\boldsymbol{e}_2 + \kappa_1\Phi_{\rm f}(\boldsymbol{q},\dot{\boldsymbol{q}})\boldsymbol{\varepsilon} + \kappa_2\boldsymbol{\xi}) \tag{29}$$

in which $\Gamma \in \mathbb{R}^{N\times N}$ is a positive-definite diagonal matrix of learning rates, and κ_1, $\kappa_2 \in \mathbb{R}^+$ are weighting factors.

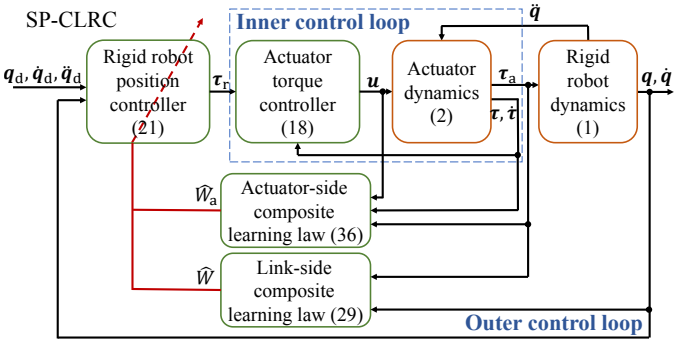

Fig. 1. A block diagram of the proposed SP-CLRC method with two-time-scale composite learning for compliant-joint robots.

The compliant actuator dynamics (2) can be rewritten into a linearly parameterized form as follows:

$$\Phi_{\rm a}^T(\ddot{\boldsymbol{\theta}})W_{\rm a} = \boldsymbol{u}(t) - \boldsymbol{\tau}_{\rm a}(t) \tag{30}$$

where $\Phi_{\rm a}(\ddot{\boldsymbol{\theta}}) := {\rm diag}(\ddot{\boldsymbol{\theta}}) \in \mathbb{R}^{n\times n}$ is an actuator-side regressor, $W_{\rm a} := [b_1, b_2, \cdots, b_n]^T \in \mathbb{R}^n$ is an actuator-side parameter vector, ${\rm diag}(\ddot{\boldsymbol{\theta}})$ is a diagonal matrix with elements $\ddot{\theta}_1$ to $\ddot{\theta}_n$, b_i is the ith diagonal element of B in (2), and $\ddot{\theta}_i$ is the ith element of $\ddot{\boldsymbol{\theta}}$ with $i = 1$ to n. To eliminate the immeasurable motor acceleration $\ddot{\boldsymbol{\theta}}$, a low-pass filter $L_\beta(s) := \frac{\beta}{s+\beta}$ with $\beta \in \mathbb{R}^+$ being a filtering constant is applied to (30) such that

$$\Phi_{\rm af}^T(\dot{\boldsymbol{\theta}})W_{\rm a} = L_\beta(s)[\boldsymbol{u}(t) - \boldsymbol{\tau}_{\rm a}(t)] := \boldsymbol{y}_{\rm f}(t) \tag{31}$$

with $\Phi_{\rm af}(\dot{\boldsymbol{\theta}}) := sL_\beta(s)[\dot{\boldsymbol{\theta}}]$. Define

$$Q(t) := \int_{t-\varsigma_{\rm a}}^{t} \Phi_{\rm af}(\varsigma)\Phi_{\rm af}^T(\varsigma)d\varsigma \tag{32}$$

with $\varsigma_{\rm a} \in \mathbb{R}^+$ being an integral duration. Multiplying (31) by $\Phi_{\rm af}$, integrating the result at $[t-\varsigma_{\rm a}, t]$, and using (32) yield

$$Q(t)W_{\rm a} = \int_{t-\varsigma_{\rm a}}^{t} \Phi_{\rm af}(\varsigma)\boldsymbol{y}_{\rm f}(\varsigma)d\varsigma := \boldsymbol{\psi}(t). \tag{33}$$

It is assumed that there exist certain constants $\sigma, \varsigma_{\rm a}, t_{\rm a} \in \mathbb{R}^+$ so that the IE condition $Q(t_{\rm a}) \geq \sigma I$ in Definition 2 is satisfied. Similarly, define a torque prediction error

$$\boldsymbol{\varepsilon}_{\rm a}(t) := \boldsymbol{y}_{\rm f}(t) - \Phi_{\rm af}^T\hat{W}_{\rm a}(t) \tag{34}$$

and a generalized torque prediction error

$$\boldsymbol{\xi}_{\rm a}(t) := \begin{cases} \boldsymbol{\psi}(t) - Q(t)\hat{W}_{\rm a}(t), & t < t_{\rm a} \\ \boldsymbol{\psi}(t_{\rm a}) - Q(t_{\rm a})\hat{W}_{\rm a}(t), & t \geq t_{\rm a} \end{cases} \tag{35}$$

where $\boldsymbol{y}_{\rm f}$ and $\boldsymbol{\psi}$ are given in (31) and (33), respectively. Design an actuator-side composite learning law

$$\dot{\hat{W}}_{\rm a} = \Gamma_{\rm a}(\Phi_{\rm af}(\dot{\boldsymbol{\theta}})\boldsymbol{\varepsilon}_{\rm a} + \kappa_3\boldsymbol{\xi}_{\rm a}) \tag{36}$$

in which $\Gamma_{\rm a} \in \mathbb{R}^{n\times n}$ is a positive-definite diagonal matrix of learning rates, and $\kappa_3 \in \mathbb{R}^+$ is a weighting factor.

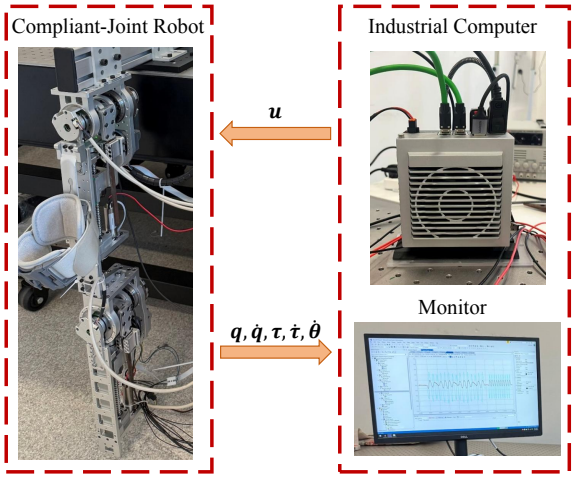

Fig. 2. A two-DoF robot driven by SEAs for experimental studies. Note that $\boldsymbol{u}$ is generated by motor outputs, $\boldsymbol{q}$, $\dot{\boldsymbol{q}}$, and $\dot{\boldsymbol{\theta}}$ are measured by position encoders, and $\boldsymbol{\tau}$ and $\dot{\boldsymbol{\tau}}$ are measured by torque sensors.

Finally, the expression of the proposed SP-CLRC composed of (18), (21), (29), and (36) is summarized by

$$\begin{cases} \boldsymbol{u} = \boldsymbol{\tau}_{\rm r} - K_{\rm p}(\boldsymbol{\tau} - \boldsymbol{\tau}_{\rm r}) - \epsilon K_{\rm d}\dot{\boldsymbol{\tau}}, \\ \boldsymbol{\tau}_{\rm r} = K_{\rm c}\boldsymbol{e}_2 + \Phi^T(\boldsymbol{q}, \dot{\boldsymbol{q}}, \dot{\boldsymbol{q}}_{\rm r}, \ddot{\boldsymbol{q}}_{\rm r})\hat{W} + \Psi_{\rm a}^T(\ddot{\boldsymbol{q}}_{\rm r})\hat{W}_{\rm a}, \\ \dot{\hat{W}} = \Gamma(\Phi(\boldsymbol{q}, \dot{\boldsymbol{q}}, \dot{\boldsymbol{q}}_{\rm r}, \ddot{\boldsymbol{q}}_{\rm r})\boldsymbol{e}_2 + \kappa_1\Phi_{\rm f}(\boldsymbol{q}, \dot{\boldsymbol{q}})\boldsymbol{\varepsilon} + \kappa_2\boldsymbol{\xi}), \\ \dot{\hat{W}}_{\rm a} = \Gamma_{\rm a}(\Phi_{\rm af}(\dot{\boldsymbol{\theta}})\boldsymbol{\varepsilon}_{\rm a} + \kappa_3\boldsymbol{\xi}_{\rm a}) \end{cases} \tag{37}$$

where $\Psi_{\rm a}(\ddot{\boldsymbol{q}}_{\rm r}) := (I + K_{\rm p})^{-1}{\rm diag}(\ddot{\boldsymbol{q}}_{\rm r}) \in \mathbb{R}^{n\times n}$ is an actuator-side generalized regressor, and $\Psi^T(\boldsymbol{q}, \dot{\boldsymbol{q}}, \dot{\boldsymbol{q}}_{\rm r}, \ddot{\boldsymbol{q}}_{\rm r})\hat{W}_{\rm e}$ in (21) is replaced by $\Phi^T(\boldsymbol{q}, \dot{\boldsymbol{q}}, \dot{\boldsymbol{q}}_{\rm r}, \ddot{\boldsymbol{q}}_{\rm r})\hat{W} + \Psi_{\rm a}^T(\ddot{\boldsymbol{q}}_{\rm r})\hat{W}_{\rm a}$ as $\Psi(\boldsymbol{q}, \dot{\boldsymbol{q}}, \dot{\boldsymbol{q}}_{\rm r}, \ddot{\boldsymbol{q}}_{\rm r}) = [\Phi^T(\boldsymbol{q}, \dot{\boldsymbol{q}}, \dot{\boldsymbol{q}}_{\rm r}, \ddot{\boldsymbol{q}}_{\rm r}), \Psi_{\rm a}^T(\ddot{\boldsymbol{q}}_{\rm r})]^T$. The closed-loop control diagram is shown in Fig. 1. It follows from the theoretical result in [24] that for the robotic system (1)–(2) under Properties 1–4 driven by the SP-CLRC law (37), if there exist constants σ, $\varsigma_{\rm e}$, $\varsigma_{\rm a}$, $t_{\rm e}$, $t_{\rm a} \in \mathbb{R}^+$ such that the IE conditions $\Theta(t_{\rm e}) \geq \sigma I$ and $Q(t_{\rm a}) \geq \sigma I$ in Definition 2 hold, the closed-loop system composed of (1), (2), and (37) achieves practical exponential stability in the sense that the tracking error $\boldsymbol{e}_1$ exponentially converges to a small neighborhood of $\mathbf{0}$ subject to the small constant ϵ, and the estimation errors $\tilde{W}(t) := W - \hat{W}(t)$ and $\tilde{W}_{\rm a}(t) := W_{\rm a} - \hat{W}_{\rm a}(t)$ exponentially converge to $\mathbf{0}$.

Compared with the latest SP-CLRC methods of compliant-joint robots in [23], [24], the proposed method has two significant distinctions: 1) It estimates the link-side parameter W in (3) and the actuator-side parameter $W_{\rm a}$ in (30) by using the composite learning laws (29) and (36), respectively, whereas existing methods directly estimate the coupled parameter $W_{\rm e}$ in (20); 2) it only uses the physically available states $\boldsymbol{q}$, $\dot{\boldsymbol{q}}$, $\boldsymbol{\tau}$, $\dot{\boldsymbol{\tau}}$, and $\dot{\boldsymbol{\theta}}$, rather than the physically unavailable states $\bar{\boldsymbol{q}}$ and $\dot{\bar{\boldsymbol{q}}}$, to achieve the estimaton error $\tilde{W}_{\rm e}$ converging to $\mathbf{0}$.

V. Experimental Verification

A two-DoF compliant-joint robot driven by SEAs in Fig. 2 is utilized for experimental validation [30]. The SEA is equipped with a joint torque sensor (M2210A2, Sunrise Instruments (SRI)) and magnetic encoders (Orbis, Renishaw PLC). An

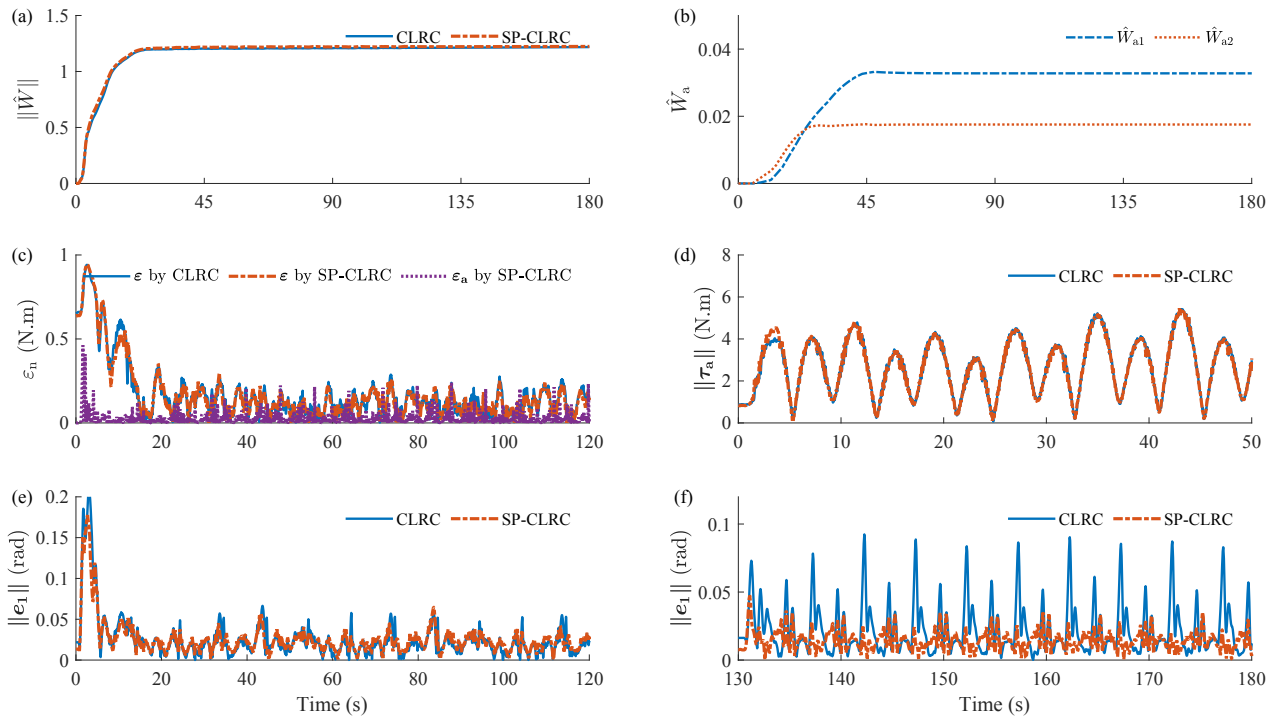

Fig. 3. Online identification and control results by two controllers in experiments. (a) Link-side parameter estimate norms $\|\hat{W}\|$. (b) Actuator-side parameter estimate $\hat{W}_a$ (by the proposed SP-CLRC only). (c) Normalized prediction errors ε_n in Task 1. (d) Actuation torque norms $\|\boldsymbol{\tau}_a\|$ in Task 1. (e) Tracking error norms $\|\boldsymbol{e}_1\|$ in Task 1 (under learning). (f) $\|\boldsymbol{e}_1\|$ in Task 2 (after learning). Note that $\hat{W}_{ai}$ with $i = 1, 2$ is the ith element of $\hat{W}_a$, and $\varepsilon_n := x/\sqrt{(a + x^2)}$ ($x = \|\boldsymbol{\varepsilon}\|$ and $a = 1$ for $\boldsymbol{\varepsilon}$ in (27) and $x = \|\boldsymbol{\varepsilon}_a\|$ and $a = 0.1$ for $\boldsymbol{\varepsilon}_a$ in (34)).

industrial computer (C6030, Beckhoff Automation GmbH & Co. KG) embedded with Beckhoff TwinCAT 3 software is used to implement real-time control. The sampling frequency of the robot control system is set at 1 kHz. To verify the superiority of the proposed SP-CLRC in both online identification and control, we choose a state-of-the-art CLRC method presented [23] as a baseline, where its expression is given by

$$\begin{cases} \boldsymbol{u} = \boldsymbol{\tau}_r - K_p(\boldsymbol{\tau} - \boldsymbol{\tau}_r) - \epsilon K_d \dot{\boldsymbol{\tau}}, \\ \boldsymbol{\tau}_r = K_c \boldsymbol{e}_2 + \Phi^T(\boldsymbol{q}, \dot{\boldsymbol{q}}, \dot{\boldsymbol{q}}_r, \ddot{\boldsymbol{q}}_r)\hat{W}, \\ \dot{\hat{W}} = \Gamma(\Phi(\boldsymbol{q}, \dot{\boldsymbol{q}}, \dot{\boldsymbol{q}}_r, \ddot{\boldsymbol{q}}_r)\boldsymbol{e}_2 + \kappa_1 \Phi_f(\boldsymbol{q}, \dot{\boldsymbol{q}})\boldsymbol{\varepsilon} + \kappa_2 \boldsymbol{\xi}) \end{cases} \tag{38}$$

which considers only the uncertainty in the link-side dynamics (1) and achieves parameter convergence. The existing SP-CLRC methods in [23], [24] are not compared in this study because they frequently failed to complete the experiments due to insufficient parameter convergence (please see the simulation results in [23], [24]). In (37) and (38), set inner-loop control parameters $K_p = \text{diag}(10, 5)$ and $\epsilon K_d = \text{diag}(0.08, 0.03)$, and the outer-loop control parameters $K_c = \text{diag}(4, 3)$, $\Lambda = \text{diag}(5, 4)$, $\Gamma = 0.02I$, $\Gamma_a = 0.05I$, $\kappa_1 = 0$, $\kappa_2 = \kappa_3 = 1$, $\varsigma_e = 27$ s, $\varsigma_a = 45$ s, $\alpha = 12$, and $\beta = 100$.

Experiments include two trajectory tracking tasks (Task 1 in $t \in [0, 120]$ s and Task 2 in $t \in [130, 180]$ s), and the desired joint trajectory $\boldsymbol{q}_d = [q_{d1}, q_{d2}]^T$ is given by

$$q_{d1} = \begin{cases} -\pi/6 \sin(\pi t/4) - \pi/2, t \le 120 \\ -\pi/2, 120 < t \le 130 \\ -5\pi/36 \sin(2\pi t/5) - \pi/2, 130 < t \le 180 \end{cases},$$

$$q_{d2} = \begin{cases} -0.7 \sin(\pi t/5), t \le 120 \\ 0, 120 < t \le 130 \\ -7\pi/36 \cos(2\pi t/5) + 7\pi/36, 130 < t \le 180 \end{cases}.$$

Task 1 is a training task for achieving parameter convergence of the robot, and Task 2 is a testing task for verifying its online identification and control performance.

Online identification and control results of two controllers in the experiments are exhibited in Fig. 3. For the proposed SP-CLRC, the link-side and actuator-side parameter estimates $\hat{W}$ and $\hat{W}_a$ converge to certain constants in Task 1 [see Figs. 3(a)–(b)], and the two prediction errors $\boldsymbol{\varepsilon}$ and $\boldsymbol{\varepsilon}_a$ converge rapidly in Task 1, and their norms reach around 0.2 N.m after about $t = 20$ s and 0.05 N.m after about $t = 4$ s, respectively [see Fig. 3(c)]. The two methods perform similarly on link-side parameter estimation and torque prediction during Task 1 [see Figs. 3(a) and (c)], since they utilize the same link-side composite learning law (29). The actuation torques $\boldsymbol{\tau}_a$ by the two methods in Task 1 have minor differences [see Fig. 3(d)]. Regarding the tracking performance, the proposed SP-CLRC shows similar tracking accuracy during the learning transient [see Fig. 3(e)], but significantly outperforms the baseline in Task 2 [see Fig. 3(f)], which indirectly verifies the accurate estimation of W and W_a and the necessity of considering the inner-loop information W_a during control.

VI. Conclusions

This paper has presented a feasible adaptive control strategy, termed SP-CLRC, to achieve exact online identification and

control for compliant-joint robots. The two-time-scale composite learning proposed uses only physically available robot states to achieve practical exponential stability of the closed-loop system and parameter convergence under the weak IE condition. Experiments on a two-DoF robot with SEAs have validated the theoretical results, where the proposed method significantly outperforms the baseline in online identification and control. Further work would focus on investigating the stability and robustness of the proposed method rigorously.

REFERENCES

[1] M. Zinn, O. Khatib, B. Roth, and J. K. Salisbury, "Playing it safe [human-friendly robots]," *IEEE Robot. Autom. Mag.*, vol. 11, no. 2, pp. 12–21, Jun. 2004.

[2] A. Albu-Schaffer, O. Eiberger, M. Grebenstein, S. Haddadin, C. Ott, T. Wimbock, S. Wolf, and G. Hirzinger, "Soft robotics-From torque feedback-controlled lightweight robots to intrinsically compliant systems," *IEEE Robot. Autom. Mag.*, vol. 15, no. 3, pp. 20–30, 2008.

[3] M. Laffranchi, L. Chen, N. Kashiri, J. Lee, N. G. Tsagarakis, and D. G. Caldwell, "Development and control of a series elastic actuator equipped with a semi active friction damper for human friendly robots," *Robot. Auton. Syst.*, vol. 62, no. 12, pp. 1827–1836, 2014.

[4] X. Li, Y. Pan, G. Chen, and H. Yu, "Adaptive human-robot interaction control for robots driven by series elastic actuators," *IEEE Trans. Robot.*, vol. 33, no. 1, pp. 169–182, 2017.

[5] L. Le-Tien and A. Albu-Schäffer, "Decoupling and tracking control for elastic joint robots with coupled joint structure," *Advanced Robotics*, vol. 31, no. 4, p. 184–203, 2017.

[6] Y. Pan, H. Wang, X. Li, and H. Yu, "Adaptive command-filtered backstepping control of robot arms with compliant actuators," *IEEE Trans. Control Syst. Technol.*, vol. 26, no. 3, pp. 1149–1156, May 2018.

[7] L. Le-Tien and A. Albu-Schaffer, "Robust adaptive tracking control based on state feedback controller with integrator terms for elastic joint robots with uncertain parameters," *IEEE Trans. Control Syst. Technol.*, vol. 26, no. 6, pp. 2259–2267, 2018.

[8] H. Wang, Y. Pan, S. Li, and H. Yu, "Robust sliding mode control for robots driven by compliant actuators," *IEEE Trans. Control Syst. Technol.*, vol. 27, no. 3, pp. 1259–1266, May. 2019.

[9] W. Huo, M. A. Alouane, Y. Amirat, and S. Mohammed, "Force control of SEA-based exoskeletons for multimode human-robot interactions," *IEEE Trans. Robot.*, vol. 36, no. 2, pp. 570–577, Apr. 2020.

[10] Y. Lin, H. Zhao, and H. Ding, "A data-driven approach for online path correction of industrial robots using modified flexible dynamics model and disturbance state observer," *IEEE/ASME Trans. Mechatron.*, vol. 28, no. 6, pp. 3410 – 3421, Dec. 2024.

[11] A. Giusti, J. Malzahn, N. G. Tsagarakis, and M. Althoff, "On the combined inverse-dynamics/passivity-based control of elastic-joint robots," *IEEE Trans. Robot.*, vol. 34, no. 6, pp. 1461–1471, Dec. 2018.

[12] K. Haninger and M. Tomizuka, "Robust passivity and passivity relaxation for impedance control of flexible-joint robots with inner-loop torque control," *IEEE/ASME Trans. Mechatron.*, vol. 23, no. 6, pp. 2671–2680, Dec. 2018.

[13] E. Spyrakos-Papastavridis, P. R. N. Childs, and J. S. Dai, "Passivity preservation for variable impedance control of compliant robots," *IEEE/ASME Trans. Mechatron.*, vol. 25, no. 5, pp. 2342–2353, Oct. 2020.

[14] G. C. Thomas, J. S. Mehling, J. Holley, and L. Sentis, "Phase-relaxed-passive full state feedback gain limits for series elastic actuators," *IEEE/ASME Trans. Mechatron.*, vol. 26, no. 1, pp. 586–591, Feb. 2021.

[15] H. K. Khalil, *Nonlinear Systems*, 3rd ed. Upper Saddle River, NJ, USA: Prentice Hall, 2002.

[16] B. Brogliato, R. Ortega, and R. Lozano, "Global tracking controllers for flexible-joint manipulators: A comparative study," *Automatica*, vol. 31, no. 7, pp. 941–956, 1995.

[17] X. Li, Y. Pan, G. Chen, and H. Yu, "Multi-modal control scheme for rehabilitation robotic exoskeletons," *Int. J. Robot. Res.*, vol. 36, no. 5-7, pp. 759–777, 2017.

[18] J. Kim, "Two-time scale control of flexible joint robots with an improved slow model," *IEEE Trans. Ind. Electron.*, vol. 65, no. 4, pp. 3317–3325, Apr. 2018.

[19] J. Kim and E. A. Croft, "Full-state tracking control for flexible joint robots with singular perturbation techniques," *IEEE Trans. Control Syst. Technol.*, vol. 27, no. 1, pp. 63–73, Jan. 2019.

[20] S. Han, H. Wang, and H. Yu, "Nonlinear disturbance observer-based robust motion control for multi-joint series elastic actuator-driven robots," in *Proc. IEEE Int. Conf. Robot. Autom.*, Xian, China, 2021, pp. 10 469–10 475.

[21] Y. Pan and T. Shi, "Adaptive estimation and control with online data memory: A historical perspective," *IEEE Control Syst. Lett.*, vol. 8, pp. 267–278, Feb. 2024.

[22] K. Guo and Y. Pan, "Composite adaptation and learning for robot control: A survey," *Annu. Rev. Control*, vol. 55, pp. 279–290, Dec. 2023.

[23] T. Shi, Y. Pan, and C. Wen, "Modern compliant robot control: Exploring benefits from singular perturbation synthesis," *IEEE Trans. Ind. Electron.*, vol. 72, no. 3, pp. 2758 – 2768, Mar. 2025.

[24] Y. Pan, Z. Li, T. Shi, and H. Yu, "Composite learning tracking control of high-dof compliant-joint industrial robots," *IEEE/ASME Trans. Mechatron.*, to be published, 2025, DOI: 10.1109/TMECH.2025.3599003.

[25] C. Ott, A. Albu-Schaffer, and G. Hirzinger, "Comparison of adaptive and nonadaptive tracking control laws for a flexible joint manipulator," in *IEEE/RSJ Int. Conf. Intell. Robot. Syst.*, Lausanne, Switzerland, 2002, pp. 2018–2024.

[26] M. W. Spong, S. Hutchinson, and M. Vidyasagar, *Robot Modeling and Control*, 2nd ed. New York, NY, USA: Wiley, 2020.

[27] Y. Pan and H. Yu, "Composite learning robot control with guaranteed parameter convergence," *Automatica*, vol. 89, pp. 398–406, Mar. 2018.

[28] M. W. Spong, "Adaptive control of flexible joint manipulators: Comments on two papers," *Automatica*, vol. 31, no. 4, pp. 585–590, 1995.

[29] J.-J. E. Slotine and W. Li, *Applied Nonlinear Control*. Englewood Cliffs, NJ, USA: Prentice Hall, 1991.

[30] L. Liu, S. Leonhardt, C. Ngo, and B. J. E. Misgeld, "Impedance-controlled variable stiffness actuator for lower limb robot applications," *IEEE Trans. Autom. Sci. Eng.*, vol. 17, no. 2, pp. 991–1004, Apr. 2020.